HHS Public Access

Author manuscript

J Immunol. Author manuscript; available in PMC 2017 January 15.

Published in final edited form as:

J Immunol. 2016 January 15; 196(2): 915–923. doi:10.4049/jimmunol.1500729.

Targeting ornithine decarboxylase by α-difluoromethylornithine inhibits tumor growth by impairing myeloid-derived suppressor cells

Cong Ye[¶,*,†], **Zhe Geng**[*,‡], **Donye Dominguez**[*], **Siqi Chen**[*], **Jie Fan**[*], **Lei Qin**[*], **Alan Long**[*], **Yi Zhang**[¶], **Timothy M. Kuzel**[*], and **Bin Zhang**[¶,*]

[¶]Biotherapy Center, The First Affiliated Hospital of Zhengzhou University, Zhengzhou, 450052, Henan, China

[*]Robert H. Lurie Comprehensive Cancer Center, Department of Medicine-Division of Hematology/Oncology, Northwestern University Feinberg School of Medicine, Chicago, IL 60611, USA

[†]Department of Rheumatology and Immunology, Tongji Hospital, Tongji Medical College, Huazhong University of Science and Technology, Wuhan 430030, China

[‡]Hubei Maternity and Child Health Hospital, Wuhan 430070, China

Abstract

α-difluoromethylornithine (DFMO) is currently used in chemopreventive regimens primarily for its conventional direct anti-carcinogenesis activity. However, little is known about the effect of decarboxylase (ODC) inhibition by DFMO on antitumor immune responses. We showed here that pharmacologic blockade of ODC by DFMO inhibited tumor growth in intact immunocompetent mice, but abrogated in the immunodeficient $Rag1^{-/-}$ mice, suggesting that antitumor effect of DFMO is dependent on the induction of adaptive anti-tumor T cell immune responses. Depletion of $CD8^+$ T cells impeded the tumor-inhibiting advantage of DFMO. Moreover, DFMO treatment enhanced antitumor $CD8^+$ T cell infiltration and IFN-γ production, and augmented the efficacy of adoptive T cell therapy. Importantly, DFMO impaired $Gr1^+CD11b^+$ myeloid-derived suppressor cells (MDSCs) suppressive activity through at least two mechanisms, including reducing arginase expression and activity, and inhibiting CD39/CD73-mediated pathway. MDSCs were one primary cellular target of DFMO as indicated by both adoptive transfer and MDSC depletion analyses. Our findings establish a new role of ODC inhibition by DFMO as a viable and effective immunological adjunct in effective cancer treatment, thereby adding to the growing list of chemoimmunotherapeutic applications of these agents.

Introduction

Recently, research has compellingly focused on tumor-induced immunosuppression, as tumor can escape the host immune system by fostering a highly suppressive environment

Address correspondence to: Bin Zhang, The First Affiliated Hospital of Zhengzhou University, Zhengzhou, 450052, Henan, China; Northwestern University Feinberg School of Medicine; 300 E Superior Street-Tarry 4-726; Chicago, Illinois 60611, bin.zhang@northwestern.edu, Fax: 312-503-0189; Ph: 312-503-2435.

(1-3). Immune suppression is mediated by factors released from the tumor or by infiltration of different immunosuppressive cells in the tumor microenvironment such as myeloid-derived suppressor cells (MDSCs) (4-7) or T-regulatory cells (Tregs) (8). It is believed that tilting the balance from an immune-suppressive to an immune-active environment is necessary for effective cancer therapy (9, 10). Clinical development of new therapeutics for established cancer to mitigate the tumor-induced immune suppression and help "wake up" the immune system to fight cancer is thus warranted, especially with agents with favorable toxicity profiles and mechanisms of action that differ from the currently approved checkpoint regulators.

Increased MDSC number has been shown in the blood, lymph nodes, and bone marrow of patients and animals with cancer, and to accumulate at tumor sites. These cells also suppress host anti-tumor immunity and are therefore a significant impediment to cancer immunotherapy (4-6). In mice, MDSCs are uniformly characterized by the expression of CD11b and Gr1 markers but with varied subtypes (11, 12). In parallel with tumors in mice, different human tumors are likely to induce different subtypes of MDSCs (11, 12). In metastatic melanoma, MDSCs were recently identified as a subset of $CD14^{+}$ $HLA\text{-}DR^{-/low}$ cells in PBMC that could be expanded in blood after administration of GM-CSF-based vaccines and interfere with the successful generation of DC vaccines (13). In addition, MDSCs could be responsible for the recruitment of Tregs favoring tumor growth (14). Thus, a number of treatment approaches have been suggested to overcome MDSC-induced immunosuppression (15). The main focus of these strategies is the reduction of either MDSC numbers or their immunosuppressive activity in the tumor-bearing host.

Ornithine decarboxylase (ODC) inhibitors such as α-difluoromethylornithine (DFMO) (16) were synthesized more than thirty years ago to treat facial hirsutism (excessive hair growth) and African trypanosomiasis (sleeping sickness) (17). DFMO was also found to induce tumor cell apoptosis, but its effectiveness as single therapeutic agent was modest in past clinical trials (18). So clinicians lost interest in further developing DFMO as a cancer therapeutic single-agent, but it remains in development as a putative chemopreventive agent given the polyamine-blocking ability of DFMO to hinder carcinogen-induced cancer development in a number of rodent models. The focus of this work has been in non-melanomatous skin cancer and other human epithelial cancers such as colon, esophageal, breast, and prostate malignancies (19-21). Despite the chemopreventive activity, little is known about the effect of DFMO on antitumor immune responses. Using the well-established preclinical B16 melanoma model, we showed here that pharmacologic blockade of ODC by DFMO inhibited tumor growth. The antitumor effect of DFMO is dependent on the induction of adaptive anti-tumor T cell immune responses. As DFMO impairs the suppressive function of MDSCs, our results have led to the novel application that DFMO administration may restore antitumor T cell immunity by suppressing MDSCs to limit tumor progression.

Materials and Methods

Mice, cell lines and reagents

C57BL/6 WT, Pmel trangenic and Rag1$^{-/-}$ mice were purchased from the Jackson Laboratory. Dr. Hans Schreiber (University of Chicago) provided the B16F10, B16-SIY cell lines, SIY peptides and 2C transgenic mice. CD73$^{-/-}$ mice have been described previously (22). ID8-OVA cells were generated as described previously (23). All the cell lines were routinely tested for mycoplasma infections by culture and DNA stain, and maintained in complete medium composed of RPMI 1640 with 5% FBS. All animal experiments were approved by institutional animal use committees of the Northwestern University. Eflornithine (α-difluoromethylornithine or DFMO) was purchased from AK Scientific, Inc. Dichlorofluorescin diacetate (DCFDA), and 5-fluorouracil (5-FU) were purchased from Sigma-Aldrich. CD73 selective inhibitors APCP and CD39 selective inhibitors ARL67156 were from Tocris Bioscience. Arginase 1/ARG1 Fluorescein-conjugated antibodies was purchased from R&D Systems. All the mAbs for flow cytometry were purchased from eBioscience and BioLegend. The D^{b}/gp100 tetramers were provided by the National Institutes of Health Tetramer Core Facility (Atlanta, GA). Depleting mAb clone 53.6.7 (anti-CD8α) and RB6-8C5 (anti-Gr1) antibodies were purchased from Bio X Cell. N^{ω}-hydroxy-nor-Arginine (Nor-NOHA) and arginase I activity kit were purchased from Cayman Chemical Company.

Analysis of cells by flow cytometry

All samples were initially incubated with 2.4G2 to block antibody binding to Fc receptors. Single cell suspensions were stained with 1 μg of relevant mAbs and then washed twice with cold PBS. ROS detection by DCFDA staining was conducted as described by Youn *et al.* (24). The D^{b}/gp100 tetramer staining, Foxp3 staining and intracellular IFN-γ staining were performed as previously described (22). The annexin V staining and ki67 staining were described previously (25). Intracellular Arginase 1 staining was done according to the manufacturer's instruction. Samples were conducted on a MACSQuant Analyzer (Miltenyi Biotec) and data were analyzed with FlowJo software.

ELISPOT assay

Spenic CD8^{+} T cells from tumor-bearing mice treated with or without DFMO were positively selected using IMag™ CD8a magnetic particles (BD Biosciences). Dendritic cells purified from tumor-free mice using IMag™ dendritic cell enrichment set (BD Biosciences), were incubated with above CD8^{+} T cells at a ratio of 2 to 1 in the presence or absence of gp100 peptides (1 μg/ml). The number of IFN-γ-producing cells were examined in an ELISPOT assay according to manufacturer’s protocol. The numbers and diameters of spots were counted in triplicates and calculated by an automatic ELISPOT counter.

MDSC suppressive assay

Splenic MDSCs from tumor-bearing WT or CD73$^{-/-}$ mice were selected using Gr1 or CD11b MicroBeads (Miltenyi Biotec). To generate bone marrow (BM)-derived MDSCs, BM cells were cultured with GM-CSF (40 ng/ml, Biolegend) and IL-6 (40 ng/ml,

Biolegend) in the presence or absence of DFMO at 10 mM for 4 days as previously described (24, 25). BM-derived MDSCs were enriched using CD11b or Gr1 MicroBeads (Miltenyi Biotec). Spenic $CD4^+$ T cells from tumor-free mice were positively selected using IMag™ CD4 magnetic particles (BD Biosciences), and labeled with eFluor450 dilution dye (eBioscience). Purified $CD4^+$ T cells (10^5) were subsequently incubated with irradiated $CD4^-$ splenic cells that work as antigen presenting cells (APC) and anti-CD3 (0.5 μg/ml) with or without above MDSCs (at different ratios) for 3 days. For experiments that examined the effect of arginase inhibitors, nor-NOHA (NW-hydroxyl-nor-l-arginine, 0.5 mM), were added at the beginning of the culture (25). To examine the importance of CD39/CD73 activity, MDSCs were pretreated with ARL67165 (250 μM) (26), or APCP (100 μM) (27) for 6 hours prior to the addition of T cells. T cell proliferation was measured by flow cytometric eFluor450 dye dilution.

Measurement of ODC activity

Splenic $Gr1^+CD11b^+$ cells from naïve and B16F10-bearing mice were sorted by a BD FACSAria. Cells were then homogenized and centrifuged at 100 000 *g* for 30 min at 4°C. The supernatant was harvested and assayed for ODC activity by the Ngo assay (28). ODC activity was determined by measuring the amount of putrescine (nmol) produced every 30 min (29). An aliquot of the same cell homogenate was collected for protein analysis by the Lowry assay with bovine serum albumin as a standard.

Arginase activity

Arginase activity was measured in cell lysates using the commercially available QuantiChrom Arginase Assay kit (BioAssay Systems, Hayward, USA) according to the manufacturer's instructions.

RNA extraction and real-time PCR

Total RNA was extracted using Trizol reagent (Invitrogen) according to the manufacturer's instructions. The cDNA synthesis was performed using SuperScript®One-Step RT-PCR (Invitrogen). Quantitative real-time PCR was performed to measure a series of MDSC-associated genes by SYBR Green (Bio-Rad) as previously described (25).

Tumor challenge and treatments

B16F10 or B16-SIY cells (1×10^6) in suspension were injected s.c. and ID8-OVA cells (1×10^6) in suspension were i.p. injected. DFMO was administered as a 1% solution in drinking dH_2O to mice starting 1 day after tumor injection. The mean DFMO consumption of mice was approximately 1.5 g/kg/day. Mice fed with dH_2O without DFMO were used as controls. For MDSC depletion, 2 d after tumor cell injection mice were injected i.p. by 5-FU (50 mg/kg) or anti-Gr1 antibodies (RB6-8C5, 200 μg) twice a week. Depletion of $CD8^+$ T cells was achieved by twice a week i.p. injection of depleting clone 53.6.7 (anti-CD8α, 200 μg) starting one day prior to tumor challenge. Flow cytometry confirmed depletion efficiency of target cells for 3 days following injections. For adoptive transfer of MDSCs, splenic $Gr1^+CD11b^+$ MDSCs from tumor-bearing mice purified using CD11b or Gr1 MicroBeads (Miltenyi Biotec) were injected i.v. at 5×10^6 per mouse into B16F10-bearing mice at d7

and d14. For adoptive T cell therapy, splenic 2C $CD8^+$ T cells were stimulated with 0.5 μg/ml SIY peptides and 10 ng/ml IL-2 for 2 days. These activated T cells were injected i.v. at 5×10^6 per mouse into B16-SIY-bearing mice 7 d after tumor challenge. To treat the established tumors, mice were s.c. injected with 10^6 B16F10 cells. DFMO was administered as a 1% solution in drinking water starting 7 day after tumor injection. Mice fed with dH_2O without DFMO were used as controls. Activated gp100-specific Pmel $CD8^+$ T cells at 5×10^6 per mouse were i.v. injected into tumor-bearing mice on the same day. The size of tumor was determined at 2-3 day intervals. Tumor volumes were measured along 3 orthogonal axes (a, b, and c) and calculated as abc/2.

Statistical analysis

Mean values were compared using an unpaired Student's two-tailed t test. The statistical differences between the survival of groups of mice were calculated according to the log-rank test. Probability values >0.05 were considered non-significant.

Results

Antitumor effect of DFMO is dependent on $CD8^+$ T cells

Initial studies looked at the direct cytotoxic effect of DFMO on melanoma cell lines. As shown in **Supple. Fig. 1**, human (A375, Skemel 5 or Skemel 28) and murine (B16F10) cell lines were grown in the presence of the indicated concentrations of DFMO for a period of 3-5 days. We found that growth of all melanoma cell lines was inhibited in vitro by DMFO with some evidence of a dose effect. To investigate the effects of DFMO consumption on tumor progression *in vivo*, DFMO was fed for 2 weeks to B16F10-tumor-bearing immunocompetent mice. Mice that received DFMO showed a significant reduction of tumor growth compared to the controls (**Fig. 1A**). However, there was no significant difference of tumor growth in the immunodeficient $Rag1^{-/-}$ mice (lack of T and B lymphocytes) (**Fig. 1B**), Importantly, depletion of $CD8^+$ T cells prior to tumor challenge abrogated tumor-inhibiting advantage of DFMO in B16F10-bearing mice (**Fig. 1C**), suggesting the antitumor effect of DFMO is dependent on the induction of adaptive anti-tumor $CD8^+$ T cell immune response in addition to its direct cytotoxic effect.

DFMO treatment restores antigen-specific antitumor T cell immunity

Given the importance of immune regulation in DFMO treatment, we next examined the phenotype and cytokine profile of tumor-infiltrating immune cells in tumor-bearing mice. At 14 days after tumor inoculation, we found remarkably more tumor-infiltrating $CD8^+$ T lymphocytes in DFMO-treated mice than control mice (**Fig. 2A, B**). Tetramer staining showed a greater number of gp100-reactive (tumor-specific) $CD8^+$ T cells in DFMO-treated mice than control mice (**Fig. 2C**). Moreover, increased IFN-γ^+ cells among $CD8^+$ T cells were observed in DFMO treated mice compared with control mice (**Fig. 2D**).

To assess further the impact of DFMO treatment on antitumor T cell immunity, we used ELISPOT assays to measure per cell IFN-γ productivity of antitumor $CD8^+$ T cells stimulated by dendritic cells pulsed with gp100 peptides. As expected, the numbers of antigen-induced IFN-γ spots increased when the $CD8^+$ T cells from DFMO-treated B16F10-

bearing mice were compared with those from control mice (**Fig. 3A, B**). This corresponds to a frequency increase of IFN-γ^+CD8$^+$ T cells by flow cytometry (**Fig. 2D**). The digital image analysis showed that the total diameter of spots (**Fig. 3C**) and mean spot size (**Fig. 3D**) were also significantly increased following DFMO treatment. These data suggest that inhibition of ODC by DFMO enhanced antitumor T-cell immunity that may contribute to the inhibition of tumor growth.

DFMO impairs MDSC activity through an arginase-mediated mechanism

In search of a cellular mechanism for the DFMO-mediated antitumor effect we investigated the well-defined immunosuppressive immune cell subsets in tumor, including MDSCs and Tregs. We found that DFMO treatment failed to affect the accumulation of splenic and intratumoral CD4$^+$Foxp3$^+$ Tregs (**Supple. Fig. 2A**). Moreover, there was no significant alteration in the expression of various Treg-associated markers, including CD39, CD73, GITR and CTLA-4, and Foxp3 on these Tregs between DFMO-treated mice and control mice (**Supple. Fig. 2B and C**). Similar to Tregs, the percentages of both splenic and intratumoral Gr1$^+$CD11b$^+$ MDSCs were nearly comparable between the control mice and DFMO-treated mice (**Fig. 4A and B**). MDSCs consist of ly6G$^-$ly6C^{high} (monocytic) and ly6G$^+$ly6C^{low}(granulocytic) subpopulations (24, 30). No significant differences in both granulocytic and monocytic MDSC subsets were further found between DFMO-treated mice and control mice, while there was a trend towards alteration of intratumor M/G-MDSC ratio (**Fig. 4B**). There was a higher ODC activity in Gr1$^+$CD11b$^+$ MDSCs from tumor-bearing mice than those from naïve mice. As expected, DFMO treatment inhibited the ODC activity in MDSCs from tumor-bearing mice (**Fig. 4C**). We next examined the phenotypes of MDSCs in tumor-bearing mice. MDSCs from DFMO-treated mice had similar levels of MHC-II, B7H1 (PD-L1) and ROS compared with those from control mice. However, significantly decreased expression of CD39, CD73, CD115 (M-CSFR) and arginase-I was observed in monocytic MDSCs from DFMO-treated mice (**Fig. 4D**).

To examine whether DFMO directly affect MDSC differentiation, we generated MDSCs in short term culture *in vitro* from BM precursor cells in the absence or presence of DFMO using GM-CSF and IL-6 cytokines (24, 25). Importantly, DFMO reduced arginase expression and activity during the induction of BM-derived MDSCs (**Fig. 5A**). Further analysis by real-time PCR revealed that *s100a9* and *mmp9* were down regulated, whereas *vegf, inos, s100a8, il1b, il12b* and *il6* were unchanged when MDSCs were treated by DFMO (**Supple. Fig. 3**). Because arginase-I in MDSCs is essential for their immunosuppressive function, we asked whether down-regulation of arginase expression and activity was implicated in the link between MDSC suppressive activity and DFMO. As expected, MDSCs without DFMO treatment inhibited T-cell proliferation in a dose-dependent manner. In sharp contrast, DFMO-treated MDSCs failed to retain their suppressive activity (**Fig. 5B**). Moreover, inhibition of arginase-I with specific inhibitor nor-NOHA completely abrogated suppressive activity of control MDSCs, whereas DFMO treatment did not affect the MDSCs (**Fig. 5B**), suggesting that DFMO impairs arginase-dependent suppressive activity of MDSCs.

To evaluate differentiation of myeloid cells in the presence of tumor-derived factors, BM cells were cultured with GM-CSF in the presence of DFMO or dH_2O as controls for 5 days in tumor cell–conditioned medium (TCM) or complete culture medium (25). We found that tumor-derived factors significantly reduced the differentiation of DCs ($CD11c^+MHC\text{-}II^+$) and macrophages ($Gr1^-F4/80^+$) and increased the generation of $Gr1^+CD11b^+$ MDSCs in WT populations (**Supple. Fig. 2D**), consistent with our previous observation (25). However, there was no significant difference of myeloid cell differentiation between DFMO treatment and the control group (**Supple. Fig. 2D**), excluding a potential effect of DFMO in MDSC differentiation in the tumor microenvironment.

DFMO impairs MDSC activity through a CD39/CD73-mediated mechanism

We showed that BM-induced G-MDSC subset expressed higher levels of CD73 than M-MDSC subset, while CD39 and CD115 (M-CSFR) were expressed predominantly in M-MDSC (**Fig. 6A and B**), in line with previous studies (27, 31). Notably, DFMO treatment decreased expression levels of CD39 and CD115 in M-MDSC subset, and CD73 in both MDSC subsets (**Fig. 6A and B**). To define the importance of CD73/CD39 in MDSCs for their immunosuppressive function, we incubated WT or $CD73^{-/-}$ MDSCs from tumor-bearing mice with T cells. The $CD73^{-/-}$ MDSCs had reduced capacity to suppress T cell proliferation, compared to WT MDSCs (**Fig. 6C**). Furthermore, inhibition of CD39 or CD73 enzymatic activity in MDSC by ARL67156 or APCP inhibitors also diminished the suppressive function of WT MDSCs (**Fig. 6C**), whereas DFMO treatment did not affect the suppressive function of $CD73^{-/-}$ MDSCs (**Fig. 6D**). These results suggest that DFMO may reduce CD73/CD39 expression and activity on MDSCs, thereby weakening their suppressive function.

DFMO modulates MDSCs to inhibit tumor growth

In addition to the B16F10 melanoma model, we showed that DFMO treatment was also effective to increase the survival of ID8-OVA ovarian tumor-bearing mice (**Supple. Fig. 4A**). Moreover, MDSCs from DFMO-treated tumor-bearing mice impaired their suppressive activity compared to those from control mice (**Supple. Fig. 4B**). We next tested whether DFMO inhibited tumor growth in an MDSC-dependent manner. We initially performed MDSC depletion in tumor-bearing mice using 5-FU (**Fig. 7A**) or anti-Gr1 antibodies (**Fig. 7B**). Consistent with prior published data (25, 32, 33), we confirmed that either 5-FU or anti-Gr1 antibodies efficiently depleted $CD11b^+Gr1^+$ populations within tumor-bearing mice (data not shown). Notably, MDSC depletion greatly inhibited tumor growth in control mice, indicating a tumor-promoting role for MDSCs. By contrast, MDSC depletion minimally affected tumor growth in DFMO-treated mice compared to control mice (**Fig. 7A and B**). Moreover, adoptive transfer of control MDSCs into tumor-bearing mice resulted in faster tumor growth than transfer of DFMO-treated MDSCs (**Fig. 7C**), further consistent with the direct impact of DFMO on MDSCs in tumor growth. To examine the effect of MDSC on antitumor T cell accumulation, we stained with Ki67 and Annexin V to test the proliferative ability and apoptotic status of gp100-reactive (tumor-specific) $CD8^+$ T cells in the tumor. As expected, transfer of control MDSCs into tumor-bearing mice inhibited the proliferation and increased the apoptosis of tumor-infiltrating gp100-reactive $CD8^+$ T cells

(**Fig. 7D**). However, transfer of DFMO-treated MDSCs did not affect the proliferative ability and apoptotic status of gp100-reactive $CD8^+$ T cells within tumors (**Fig. 7D**). Further analysis revealed the reduced number of these tumor-specific T cells in tumor-bearing mice receiving control MDSCs rather than DFMO-treated MDSCs, as compared to mice without MDSC transfer (**Fig. 7D**). These results indicate that DFMO may inhibit tumor growth by weakening the suppressive activity of MDSCs.

DFMO treatment augments the efficacy of adoptive T-cell therapy

MDSCs suppress many import immune cells including cytotoxic $CD8^+$ T lymphocytes. Given the ability of DFMO to curtail MDSC inhibitory effect, we tested whether DFMO treatment improves the efficacy of adoptive T-cell therapy. In the B16-SIY model, transfer of high-avidity tumor-specific T-cells (SIY-specific transgenic 2C T cells) failed to limit tumor growth, while DFMO alone inihibited tumor growth (**Fig. 8A**). In the less immunogenic B16F10 model, neither transfer of gp100-specific transgenic Pmel T cells (34), nor DFMO treatment alone affected growth of established tumors (**Fig. 8B**). However, combining DFMO treatment with adoptive T-cell therapy resulted in effective antitumor effect in both models (**Fig. 8A and B**). Collectively, these data support our thesis that ODC blockade by DFMO rescues tumor-specific immunity and enhances the efficacy of adoptive T-cell therapy.

Discussion

Treatment with DFMO alone is poorly cytotoxic against tumors in vivo (19, 20). Current clinical chemoprevention trials are thus investigating the efficacy of DFMO to suppress surrogate end point biomarkers of carcinogenesis in patient populations at increased risk for the development of various epithelial cancers (19, 20). We show here that ODC inhibition by DFMO exerts an indirect immune-mediated, antitumor effect through inhibition of MDSC-mediated immunosuppressive mechanisms.

Using the well-established agressive B16 melanoma model, we demonstrate that pharmacologic blockade of ODC by DFMO inhibited tumor growth, consistent with the previous observations (35, 36). Besides the anti-proliferative action, our findings establish a new role for ODC inhibition by DFMO as a viable and effective immunological modulator in cancer treatment. This novel mechanism of action has been hypothesized on the basis of several lines of evidence. First, the anti-tumor effect of DFMO is observed in intact immunocompetent mice, but abrogated in the immunodeficient $Rag1^{-/-}$ mice. Second, depletion of $CD8^+$ T cells prior to tumor challenge impedes the tumor-inhibiting advantage of DFMO. Third, DFMO treatment enhances antitumor $CD8^+$ T cell infiltration and IFN-γ production, and augments the efficacy of adoptive T cell therapy. Fourth, DFMO impairs MDSC suppressive activity. Thus, DFMO may reverse tumor-induced immunosuppressive mechanisms and invoke a measurable antitumor immune response that delays cancer progression.

The importance of polyamine biosynthesis by ODC in MDSC regulation and function has not yet been characterized. To our knowledge, our data clearly provide the first evidence that DFMO restores antitumor T-cell immunity by suppressing MDSCs to limit tumor

growth, using both adoptive transfer and MDSC depletion analyses. In fact, DFMO down-regulates MDSC suppressive pathways. Moreover, DFMO reverses MDSC suppression *in vitro*. Our results indicate $Gr1^+CD11b^+$ MDSCs are one primary cellular target of DFMO. However, we did not detect changes in the MDSC accumulation following DFMO treatment. In addition, no significant differences in both granulocytic and monocytic MDSC subsets were further found in the treated mice. A recent study has reported that a novel polyamine-blocking therapy that combines DFMO and AMXT 1501 as an inhibitor of polyamine transport, decreased levels of tumor-infiltrating $Gr1^+CD11b^+$ cells, and inhibited the M2 polarization of myeloid cells (37). It remains to be defined whether the use of polyamine transport inhibitors would be required to impair the accumulation and function of MDSCs together with DFMO. Moreover, DFMO-mediated antitumor effects on other immune cells (e.g. NK cells and macrophages) need to be explored.

In an effort to unravel the molecular basis for DFMO-mediated inhibitory effect on MDSC activity, we found that DFMO reduced arginase expression and activity to weaken the suppressive activity of MDSCs. Recent findings in tumor bearing mice and cancer patients indicate that the enhanced metabolism of L-Arginine by MDSC producing Arginase I inhibits T-cell responses (38). L-arginine is the major precursor through the sequential actions of arginase, which leads to L-ornithine generation and ODC. L-ornithine is a substrate for ODC, and has been shown to retroinhibit arginase (39). As DFMO is a structural analogue of L-ornithine, there is likely a direct effect of this reagent upon arginase. Indeed, it was demonstrated that DFMO could be used as a potent arginase activity inhibitor in human cancer cells (40). Another study has reported that increased polyamine levels induce arginase activity in epithelial cells and DFMO blocks the IL-4–induced arginase activity of macrophages (37). Although our data expand the effect of DFMO to MDSC-mediated tumor protection, the inhibitory effect of DFMO on arginase expression and activity in both immune and non-immune conditions needs further investigation.

In addition to regulating the metabolism of L-Arginine, DFMO reduced levels of CD39 and CD73 that act as functional markers for MDSCs. The frequency and function of MDSCs could be modulated by extracellular adenosine (41). Notably, we showed that the MDSCs immunosuppressive activity was at least partially dependent on CD39/CD73-mediated adenosinergic effect, suggesting a connection between DFMO and CD39/CD73-mediated pathway to reverse MDSC function. On the other hand, MDSCs also promote tumor progression through non-immune mechanisms. Their release of MMP-9 stimulates tumor angiogenesis. Given the decreased production of MMP-9 from DFMO-treated MDSCs, further studies will determine whether DFMO affects MDSC-dependent tumor angiogenesis.

Because DFMO administration inhibited MDSC activity and was associated with restored T-lymphocyte activity, we reasoned that it may create a favorable environment for effective immunotherapy. Our preclinical studies reveal the feasibility of targeting ODC using DFMO to control tumor progression by unmasking anti-tumor T-cell immune responses. This novel strategy likely requires the weakening of tumor-induced immune suppression that is mediated by MDSCs. However, endogenous immunity that can be restored is often insufficient and transient. Thus, targeting ODC using DFMO may be more effective combined with other immunotherapies, such as adoptive T-cell transfer, immune-stimulating

mAbs or DC vaccines. In support of this concept, in this study we demonstrated that the therapeutic efficacy of adoptively transferred tumor antigen-specific T-cells was significantly enhanced by DFMO administration, resulting in regression of aggressive B16 melanoma.

Compared with the other chemotherapeutic drugs assessed for MDSC inhibition, DFMO is endowed with a high degree of safety and tolerability, and is relatively inexpensive. DFMO is currently used in chemopreventive regimen primarily for its conventional direct anti-carcinogenesis activity. Here we highlight a new application for this drug as a potent immunomodulatory agent, which can be used to overcome a major mechanism of tumor immune evasion by targeting MDSCs. These observations open the opportunity for the rapid translation of our preclinical findings into the clinic and advocate for the implementation of polyamine-blocking agent in combination strategies to enhance the efficacy of immunotherapy.

Supplementary Material

Refer to Web version on PubMed Central for supplementary material.

Acknowledgments

We thank the National Institutes of Health Tetramer Facility for providing the D^b/gp100 tetramers. We thank Dr. Susan K. Gilmour for her insightful discussion.

This research was in part supported by National Institutes of Health grant CA149669, Northwestern Memorial Foundation-Friends of Prentice Grants Initiative, SPORE Pilot Award (P50 CA090386), Northwestern University RHLCCC Flow Cytometry Facility, a Cancer Center Support Grant (NCI CA060553).

References

1. Gajewski TF. Identifying and overcoming immune resistance mechanisms in the melanoma tumor microenvironment. Clin Cancer Res. 2006; 12:2326s–2330s. [PubMed: 16609053]
2. Zou W. Immunosuppressive networks in the tumour environment and their therapeutic relevance. Nat Rev Cancer. 2005; 5:263–274. [PubMed: 15776005]
3. Rabinovich GA, Gabrilovich D, Sotomayor EM. Immunosuppressive strategies that are mediated by tumor cells. Annu Rev Immunol. 2007; 25:267–296. [PubMed: 17134371]
4. Gabrilovich DI, Nagaraj S. Myeloid-derived suppressor cells as regulators of the immune system. Nat Rev Immunol. 2009; 9:162–174. [PubMed: 19197294]
5. Filipazzi P, Huber V, Rivoltini L. Phenotype, function and clinical implications of myeloid-derived suppressor cells in cancer patients. Cancer Immunol Immunother. 2012; 61:255–263. [PubMed: 22120756]
6. Ostrand-Rosenberg S. Myeloid-derived suppressor cells: more mechanisms for inhibiting antitumor immunity. Cancer Immunol Immunother. 2010; 59:1593–1600. [PubMed: 20414655]
7. Arina A, Bronte V. Myeloid-derived suppressor cell impact on endogenous and adoptively transferred T cells. Curr Opin Immunol. 2015; 33C:120–125. [PubMed: 25728992]
8. Zou W. Regulatory T cells, tumour immunity and immunotherapy. Nat Rev Immunol. 2006; 6:295–307. [PubMed: 16557261]
9. Kirkwood JM, Tarhini AA, Panelli MC, Moschos SJ, Zarour HM, Butterfield LH, Gogas HJ. Next generation of immunotherapy for melanoma. J Clin Oncol. 2008; 26:3445–3455. [PubMed: 18612161]

10. Postow MA, Harding J, Wolchok JD. Targeting immune checkpoints: releasing the restraints on anti-tumor immunity for patients with melanoma. Cancer J. 2012; 18:153–159. [PubMed: 22453017]
11. Peranzoni E, Zilio S, Marigo I, Dolcetti L, Zanovello P, Mandruzzato S, Bronte V. Myeloid-derived suppressor cell heterogeneity and subset definition. Curr Opin Immunol. 2011; 22:238–244. [PubMed: 20171075]
12. Youn JI, Gabrilovich DI. The biology of myeloid-derived suppressor cells: the blessing and the curse of morphological and functional heterogeneity. Eur J Immunol. 2011; 40:2969–2975. [PubMed: 21061430]
13. Filipazzi P, Valenti R, Huber V, Pilla L, Canese P, Iero M, Castelli C, Mariani L, Parmiani G, Rivoltini L. Identification of a new subset of myeloid suppressor cells in peripheral blood of melanoma patients with modulation by a granulocyte-macrophage colony-stimulation factor-based antitumor vaccine. J Clin Oncol. 2007; 25:2546–2553. [PubMed: 17577033]
14. Schlecker E, Stojanovic A, Eisen C, Quack C, Falk CS, Umansky V, Cerwenka A. Tumor-infiltrating monocytic myeloid-derived suppressor cells mediate CCR5-dependent recruitment of regulatory T cells favoring tumor growth. J Immunol. 2012; 189:5602–5611. [PubMed: 23152559]
15. Umansky V, Sevko A. Melanoma-induced immunosuppression and its neutralization. Seminars in cancer biology. 2012; 22:319–326. [PubMed: 22349515]
16. Kehe CR, Harris JW. Ornithine decarboxylase and polyamines in the resumption of cycling by diluted and reoxygenated mammalian cells. Exp Cell Res. 1978; 115:405–408. [PubMed: 689095]
17. Milord F, Pepin J, Loko L, Ethier L, Mpia B. Efficacy and toxicity of eflornithine for treatment of Trypanosoma brucei gambiense sleeping sickness. Lancet. 1992; 340:652–655. [PubMed: 1355219]
18. Casero RA Jr. Marton LJ. Targeting polyamine metabolism and function in cancer and other hyperproliferative diseases. Nat Rev Drug Discov. 2007; 6:373–390. [PubMed: 17464296]
19. Gerner EW, Meyskens FL Jr. Polyamines and cancer: old molecules, new understanding. Nat Rev Cancer. 2004; 4:781–792. [PubMed: 15510159]
20. Meyskens FL Jr. Gerner EW. Development of difluoromethylornithine (DFMO) as a chemoprevention agent. Clin Cancer Res. 1999; 5:945–951. [PubMed: 10353725]
21. Babbar N, Gerner EW. Targeting polyamines and inflammation for cancer prevention. Recent results in cancer research. Fortschritte der Krebsforschung. Progres dans les recherches sur le cancer. 2011; 188:49–64. [PubMed: 21253788]
22. Wang L, Fan J, Thompson LF, Zhang Y, Shin T, Curiel TJ, Zhang B. CD73 has distinct roles in nonhematopoietic and hematopoietic cells to promote tumor growth in mice. J Clin Invest. 2011; 121:2371–2382. [PubMed: 21537079]
23. Jin D, Fan J, Wang L, Thompson LF, Liu A, Daniel BJ, Shin T, Curiel TJ, Zhang B. CD73 on tumor cells impairs antitumor T-cell responses: a novel mechanism of tumor-induced immune suppression. Cancer Res. 2010; 70:2245–2255. [PubMed: 20179192]
24. Youn JI, Nagaraj S, Collazo M, Gabrilovich DI. Subsets of myeloid-derived suppressor cells in tumor-bearing mice. J Immunol. 2008; 181:5791–5802. [PubMed: 18832739]
25. Chen S, Wang L, Fan J, Ye C, Dominguez D, Zhang Y, Curiel TJ, Fang D, Kuzel TM, Zhang B. Host miR155 promotes tumor growth through a myeloid-derived suppressor cell-dependent mechanism. Cancer Res. 2015; 75:519–531. [PubMed: 25502838]
26. Borsellino G, Kleinewietfeld M, Di Mitri D, Sternjak A, Diamantini A, Giometto R, Hopner S, Centonze D, Bernardi G, Dell'Acqua ML, Rossini PM, Battistini L, Rotzschke O, Falk K. Expression of ectonucleotidase CD39 by Foxp3+ Treg cells: hydrolysis of extracellular ATP and immune suppression. Blood. 2007; 110:1225–1232. [PubMed: 17449799]
27. Ryzhov S, Novitskiy SV, Goldstein AE, Biktasova A, Blackburn MR, Biaggioni I, Dikov MM, Feoktistov I. Adenosinergic regulation of the expansion and immunosuppressive activity of CD11b+Gr1+ cells. J Immunol. 2011; 187:6120–6129. [PubMed: 22039302]
28. Ngo TT, Brillhart KL, Davis RH, Wong RC, Bovaird JH, Digangi JJ, Ristow JL, Marsh JL, Phan AP, Lenhoff HM. Spectrophotometric assay for ornithine decarboxylase. Analytical biochemistry. 1987; 160:290–293. [PubMed: 3578755]

29. Ma Q, Wang Y, Gao X, Ma Z, Song Z. L-arginine reduces cell proliferation and ornithine decarboxylase activity in patients with colorectal adenoma and adenocarcinoma. Clin Cancer Res. 2007; 13:7407–7412. [PubMed: 18094424]
30. Movahedi K, Guilliams M, Van den Bossche J, Van den Bergh R, Gysemans C, Beschin A, De Baetselier P, Van Ginderachter JA. Identification of discrete tumor-induced myeloid-derived suppressor cell subpopulations with distinct T cell-suppressive activity. Blood. 2008; 111:4233–4244. [PubMed: 18272812]
31. Huang B, Pan PY, Li Q, Sato AI, Levy DE, Bromberg J, Divino CM, Chen SH. Gr-1+CD115+ immature myeloid suppressor cells mediate the development of tumor-induced T regulatory cells and T-cell anergy in tumor-bearing host. Cancer Res. 2006; 66:1123–1131. [PubMed: 16424049]
32. Tomihara K, Guo M, Shin T, Sun X, Ludwig SM, Brumlik MJ, Zhang B, Curiel TJ, Shin T. Antigen-specific immunity and cross-priming by epithelial ovarian carcinoma-induced CD11b(+)Gr-1(+) cells. J Immunol. 2010; 184:6151–6160. [PubMed: 20427766]
33. Vincent J, Mignot G, Chalmin F, Ladoire S, Bruchard M, Chevriaux A, Martin F, Apetoh L, Rebe C, Ghiringhelli F. 5-Fluorouracil selectively kills tumor-associated myeloid-derived suppressor cells resulting in enhanced T cell-dependent antitumor immunity. Cancer Res. 2010; 70:3052–3061. [PubMed: 20388795]
34. Overwijk WW, Theoret MR, Finkelstein SE, Surman DR, de Jong LA, Vyth-Dreese FA, Dellemijn TA, Antony PA, Spiess PJ, Palmer DC, Heimann DM, Klebanoff CA, Yu Z, Hwang LN, Feigenbaum L, Kruisbeek AM, Rosenberg SA, Restifo NP. Tumor regression and autoimmunity after reversal of a functionally tolerant state of self-reactive CD8+ T cells. J Exp Med. 2003; 198:569–580. [PubMed: 12925674]
35. Bowlin TL, Hoeper BJ, Rosenberger AL, Davis GF, Sunkara PS. Effects of three irreversible inhibitors of ornithine decarboxylase on macrophage-mediated tumoricidal activity and antitumor activity in B16F1 tumor-bearing mice. Cancer Res. 1990; 50:4510–4514. [PubMed: 2114941]
36. Bowlin TL, McKown BJ, Davis GF, Sunkara PS. Effect of polyamine depletion in vivo by DL-alpha-difluoromethylornithine on functionally distinct populations of tumoricidal effector cells in normal and tumor-bearing mice. Cancer Res. 1986; 46:5494–5498. [PubMed: 3093066]
37. Hayes CS, Shicora AC, Keough MP, Snook AE, Burns MR, Gilmour SK. Polyamine-blocking therapy reverses immunosuppression in the tumor microenvironment. Cancer immunology research. 2014; 2:274–285. [PubMed: 24778323]
38. Raber P, Ochoa AC, Rodriguez PC. Metabolism of L-arginine by myeloid-derived suppressor cells in cancer: mechanisms of T cell suppression and therapeutic perspectives. Immunol Invest. 2012; 41:614–634. [PubMed: 23017138]
39. Reczkowski RS, Ash DE. Rat liver arginase: kinetic mechanism, alternate substrates, and inhibitors. Arch Biochem Biophys. 1994; 312:31–37. [PubMed: 8031143]
40. Selamnia M, Mayeur C, Robert V, Blachier F. Alpha-difluoromethylornithine (DFMO) as a potent arginase activity inhibitor in human colon carcinoma cells. Biochemical pharmacology. 1998; 55:1241–1245. [PubMed: 9719479]
41. Iannone R, Miele L, Maiolino P, Pinto A, Morello S. Blockade of A2b adenosine receptor reduces tumor growth and immune suppression mediated by myeloid-derived suppressor cells in a mouse model of melanoma. Neoplasia. 2013; 15:1400–1409. [PubMed: 24403862]

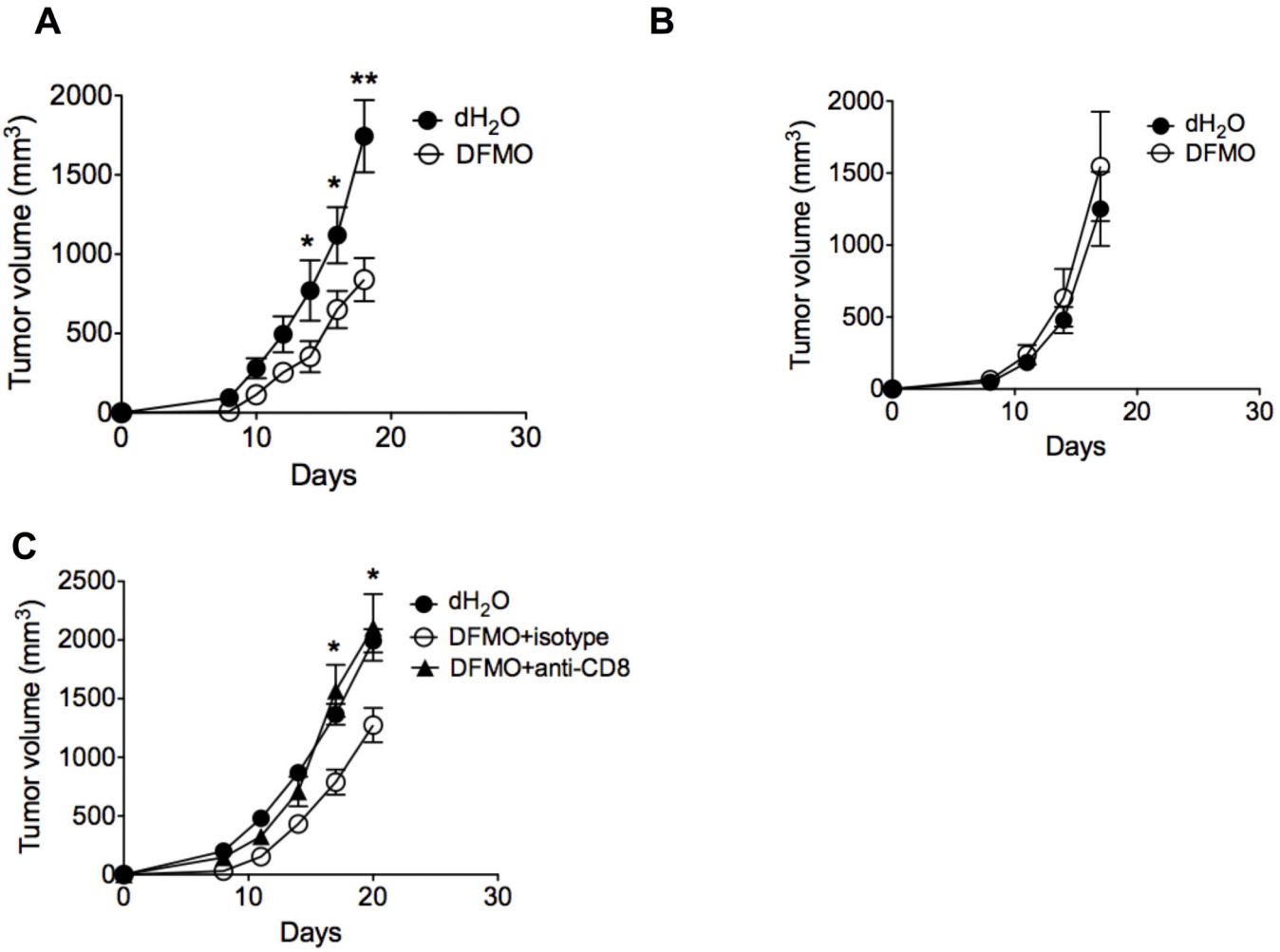

Figure 1. Antitumor effect of DFMO is dependent on CD8$^+$ T cells

B16F10 (**A, B**) or B16-SIY **(C)** cells were injected s.c. into WT **(A, C)** or Rag$^{-/-}$ C57BL/6 mice **(B)** (5 mice per group). DFMO was administered as a 1% solution in drinking dH_2O to mice starting 1 day after tumor injection. The mean DFMO consumption of mice was approximately 1.5 g/kg/day. Mice fed with dH_2O without DFMO were used as controls (5 mice per group). **(C)** Depletion of CD8$^+$ T cells was achieved by twice-weekly i.p. injection of depleting mAb clone 53.6.7 (anti-CD8α, 200 μg), starting 1 day prior to tumor challenge. Tumor volumes were measured every 2 or 3 days (5 mice per group). Data (mean ± SEM) are representative of at least 3 independent experiments. *, $p< 0.05$; **, $p<0.01$.

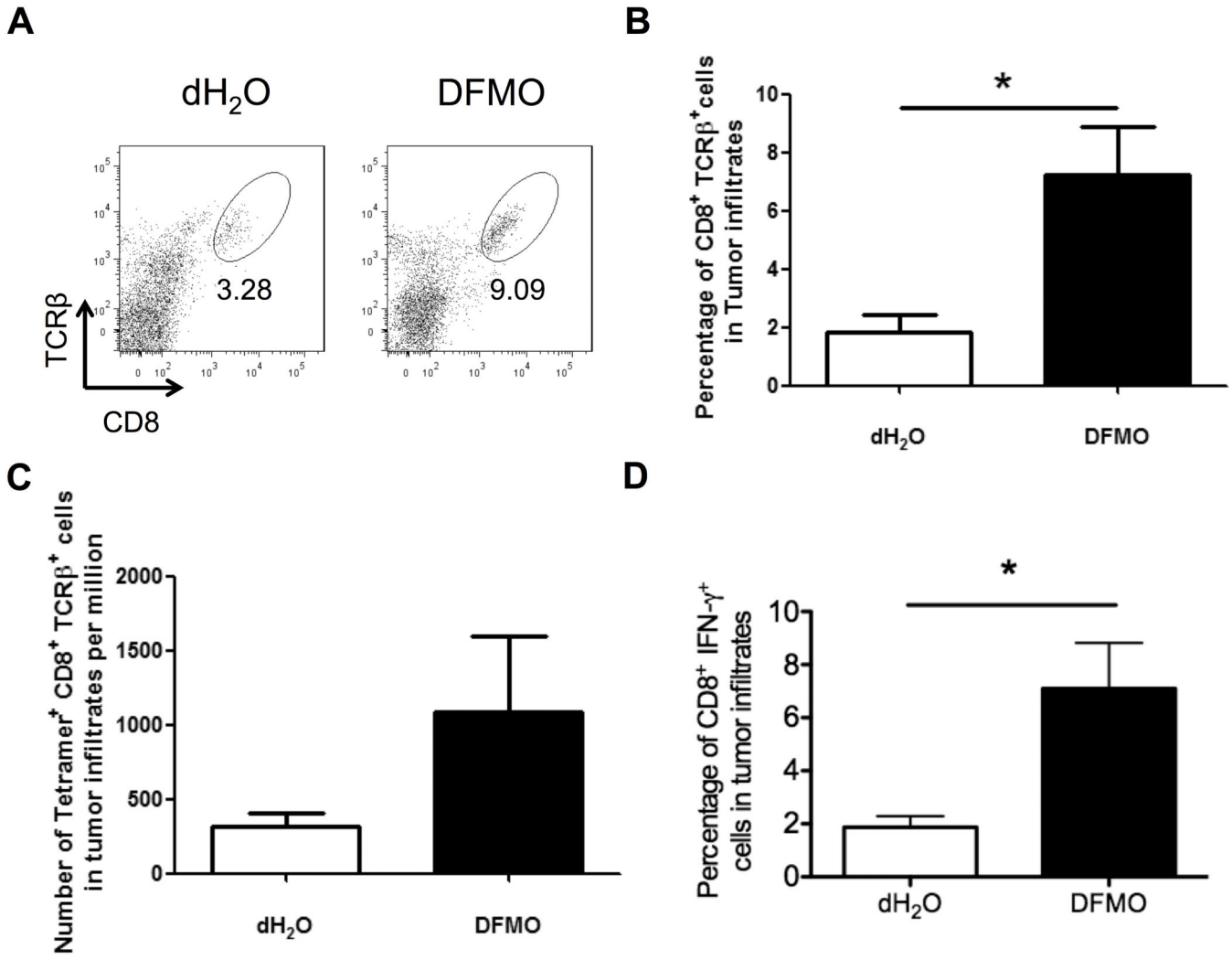

Figure 2. DFMO adminstration enhances tumor-infiltrating T cell immunity

(A) Representative flow cytometric analysis of tumor-infiltrating $CD8^+TCRV\beta^+$ T cells (5 mice per group). **(B)** Percent $CD8^+TCRV\beta^+$ cells and **(C)** absolute number of gp100-specific $tetramer^+CD8^+TCRV\beta^+$ cells per 10^6 cells in tumor infiltrates (5 mice per group). **(D)** Percent IFN-γ secreting $CD3^+CD8^+$ T cells in tumor infiltrates. Cells were collected from B16F10-bearing DFMO treated or control mice 14 days after tumor inoculation (5 mice per group). Data (mean ± SEM) are representative of 3 independent experiments. *, $p < 0.05$.

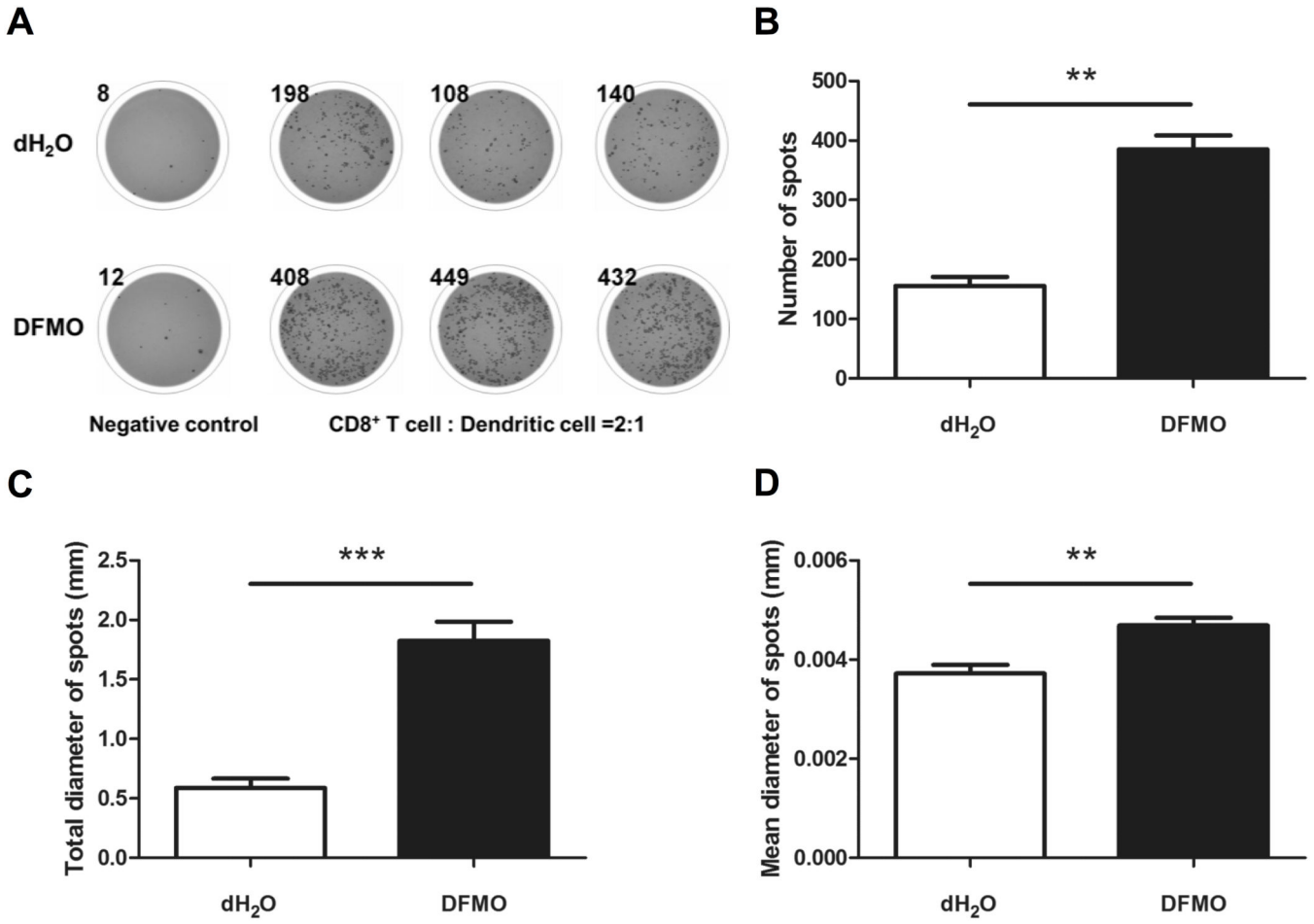

Figure 3. DFMO treatment augments IFN-γ production of CD8$^+$ T cells in response to tumor antigen

(A) Representative ELISPOT images. Negative control wells contain splenic CD8$^+$ T cells from B16F10-bearing DFMO treated or control mice collected 14 days after tumor inoculation (3 mice per group). Other triplicated wells contain CD8$^+$ T cells and dendritic cells at the ratio of 2 to 1 in the presence of tumor antigen gp100 peptides (1 μg/ml). Each spot represents an IFN-γ secreting cell. The digital image analysis showed the total number (**B**), diameter of spots (**C**) and mean spot size (**D**) were significantly increased following DFMO treatment. Data (mean ± SEM) are representative of 2 independent experiments. $^{**}p < 0.01$, $^{***}p < 0.001$.

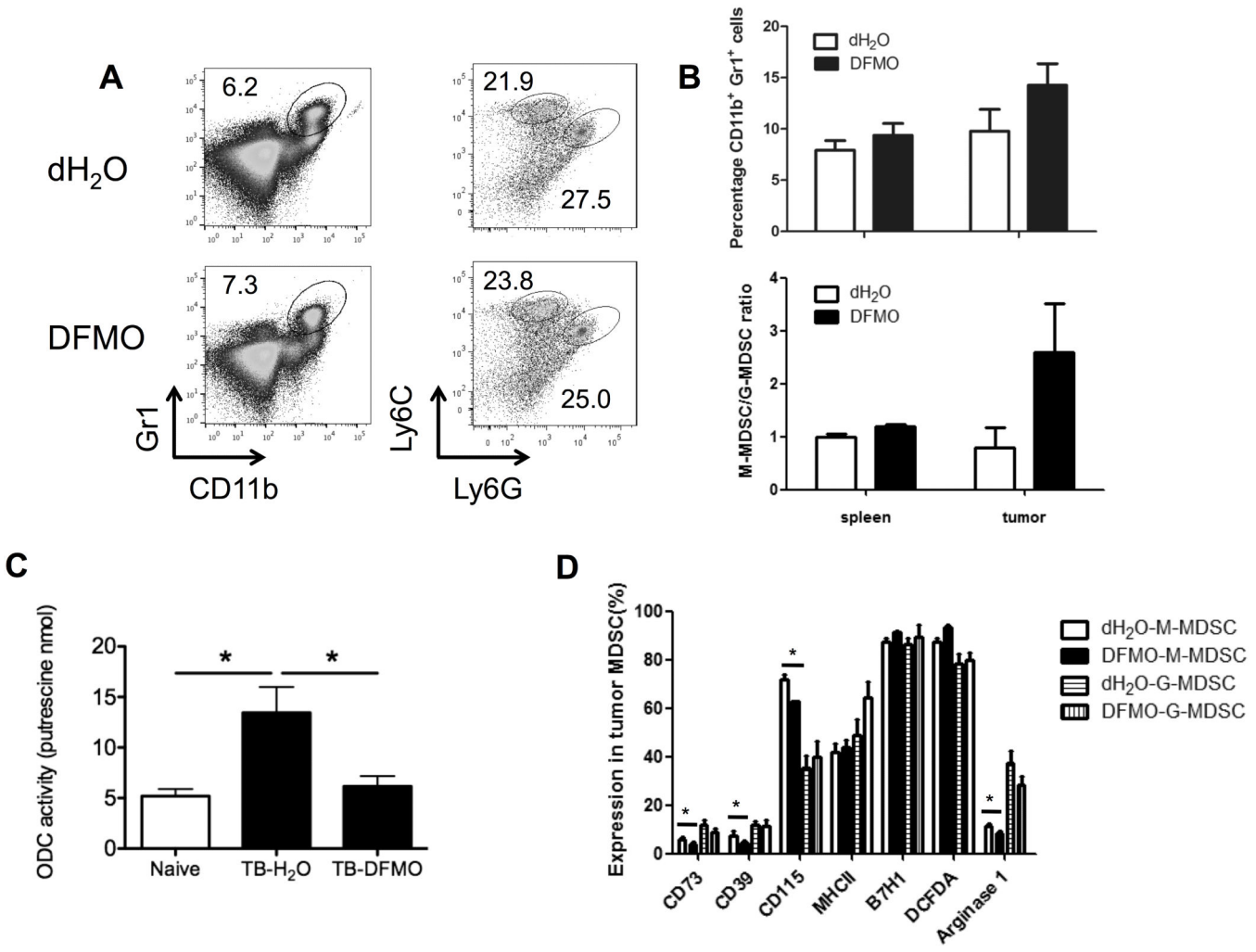

Figure 4. Charaterization of phenotypic tumor-associated MDSCs following DFMO treatment

(**A**) Percent splenic $Gr1^+CD11b^+$ MDSCs were determined by flow cytometry from B16F10-bearing mice. Percent $CD11b^+Ly6G^+Ly6C^{low}$ (granulocytic) and $CD11b^+Ly6G^-Ly6C^{high}$ (monocytic) MDSCs were indicated within plots (5 mice per group). (**B**) Percent $Gr1^+CD11b^+$ MDSCs, $CD11b^+Ly6G^+Ly6C^{low}$ (granulocytic) and $CD11b^+Ly6G^-Ly6C^{high}$ (monocytic) MDSCs in spleen and tumor tissues from B16F10-bearing mice were summarized (5 mice per group). (**C**) Measurement of ODC activity in $Gr1^+CD11b^+$ cells from naïve and B16F10 tumor-bearing (TB) mice treated by DFMO or dH_2O (5 mice per group). (**D**) Expression levels of CD39, CD73, CD115, MHC-II, B7H1, DCFDA (ROS indicator) and arginase-I among both tumor-infiltrating $CD11b^+Ly6G^+Ly6C^{low}$ (granulocytic) and $CD11b^+Ly6G^-Ly6C^{high}$ (monocytic) MDSCs were determined by flow cytometry. Cells were collected from B16F10-bearing DFMO treated or control mice 14 days after tumor inoculation (5 mice per group). Data (mean ± SEM) are representative of 2 independent experiments. *, $p < 0.05$.

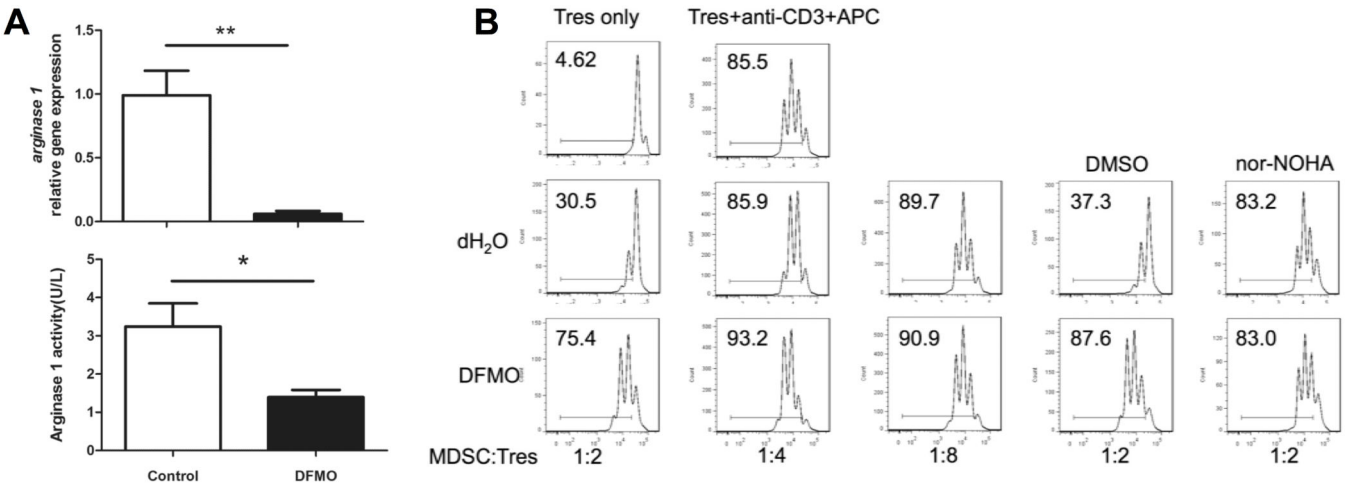

Figure 5. DFMO impairs MDSC function by reducing arginase expression and activity

(**A**) Real-time quantitative RT-PCR analysis of arginase-I expression in MDSCs from DFMO-treated and control mice (5 mice per group). Arginase-I activity of DFMO-treated MDSCs was compared with that of control MDSCs (3 mice per group). (**B**) Suppressive activity of DFMO-treated MDSCs versus control MDSCs. MDSCs were added at different ratios to eFluor450-labeled $CD4^+$ T responder cells (Tres) stimulated with anti-CD3 plus antigen-presenting cells (APC) for 3 days and T cell proliferation was measured by flow cytometric eFluor450 dye dilution (3 mice per group). Arginase-I inhibitor nor-NOHA was able to blunt the suppressive activity of control MDSC but not DFMO-treated MDSCs. *, $p<0.05$; **, $p<0.01$. Data are representative of 3 independent experiments.

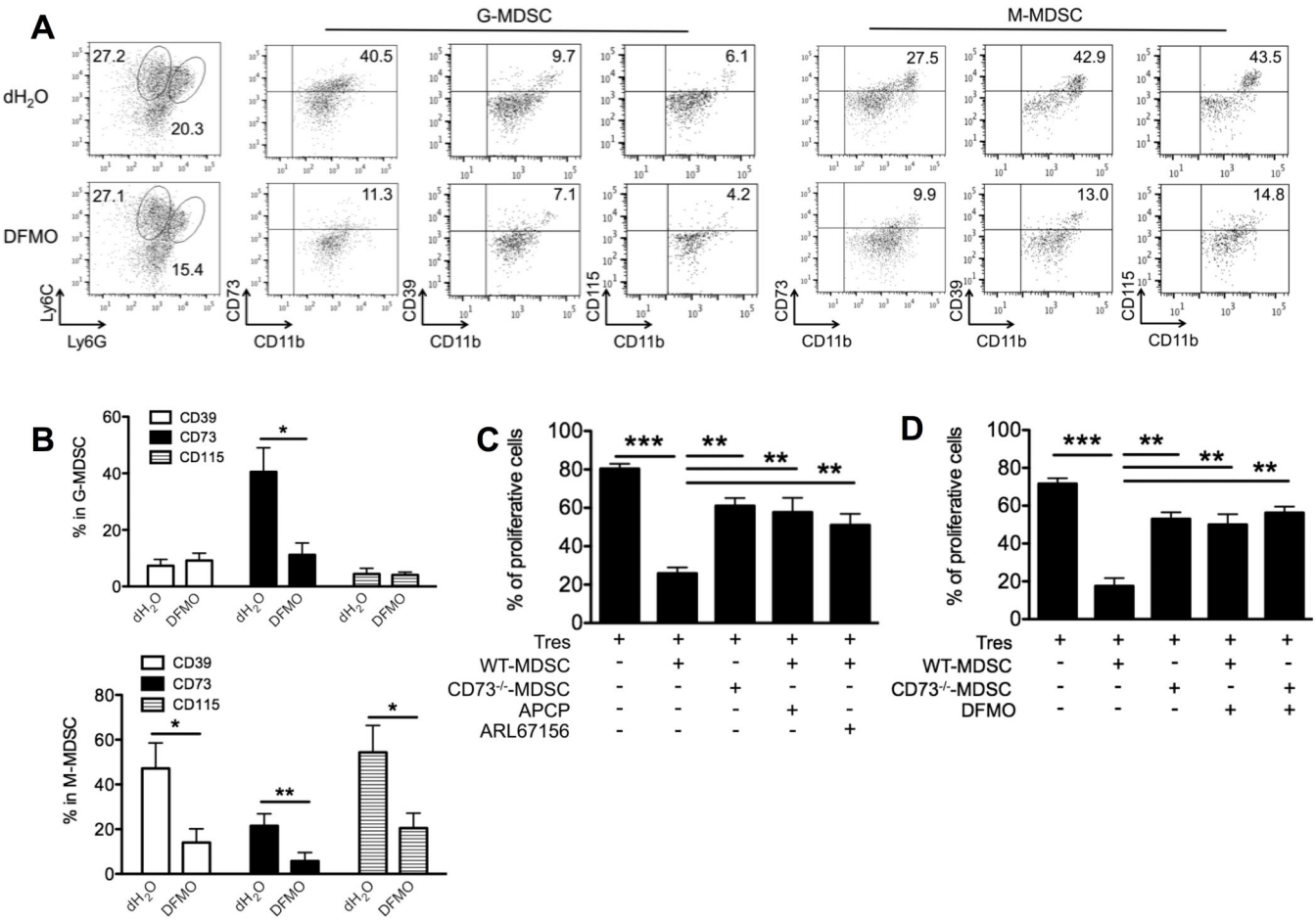

Figure 6. DFMO impairs MDSC function by reducing CD39/CD73-mediated adensinergic effect

(**A**) Representatvie flow dot plots show the gating strategy for $CD11b^{+}Ly6G^{+}Ly6C^{low}$ (granulocytic) and $CD11b^{+}Ly6G^{-}Ly6C^{high}$ (monocytic) BM-cultured MDSCs, and the percent CD73, CD39 or CD115 in each MDSC subset treated by DFMO or dH_2O as controls. (**B**) Flow quantification of CD73, CD39 or CD115 expression in DFMO-treated MDSCs versus control MDSCs (5 mice per group). *, $p<0.05$; **, $p<0.01$. (**C**) Suppressive activity of MDSCs as shown by quantification of eFluor450-labeled $CD4^{+}$ T responder cells (Tres) cocultured with the indicated $Gr1^{+}CD11b^{+}$ MDSCs treated with or without CD73 inhibitors APCP or CD39 inhibitors ARL67156. The ratio of T cell/MDSC was 2:1. (**D**) Suppressive activity of MDSCs as shown by quantification of eFluor450-labeled Tres cocultured with the indicated $Gr1^{+}CD11b^{+}$ MDSCs treated with or without DFMO. The ratio of T cell/MDSC was 2:1. **, $p<0.01$; ***, $p<0.001$ (3 mice per group). Data (mean ± SEM) are representative of 2 independent experiments.

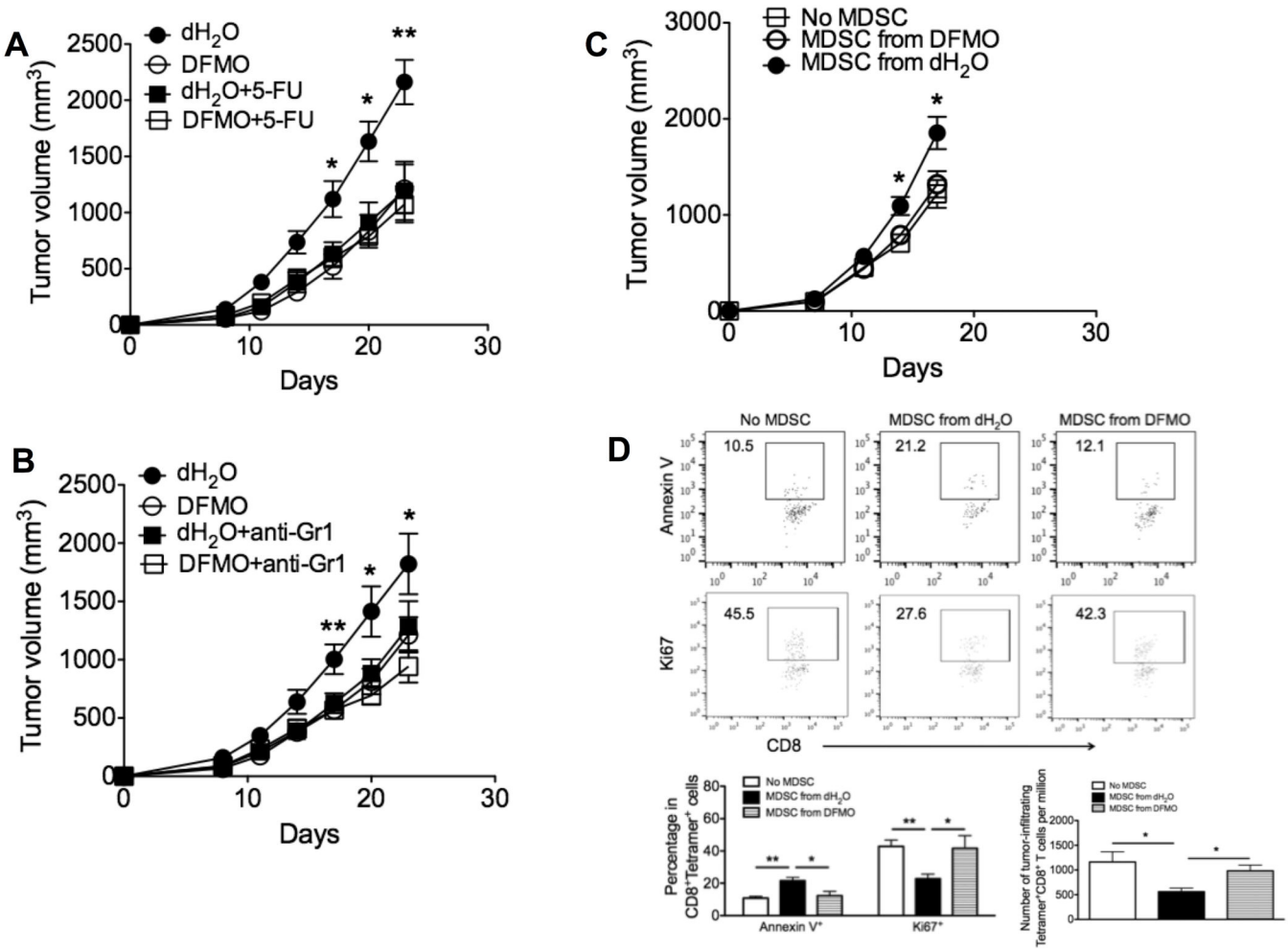

Figure 7. DFMO targets MDSCs to inhibit tumor growth

Mice were injected s.c. with 10^6 B16F10 tumor cells. Depletion of MDSC was achieved by either twice-weekly i.p. injection of (**A**) 5-Fluorouracil (5-FU) or (**B**) anti-Gr1 antibodies starting 2 days after tumor challenge (5 mice per group). (**C**) Splenic $Gr1^+CD11b^+$ MDSCs from B16F10-bearing mice treated with DFMO or dH_2O were injected i.v. into B16-bearing mice at d7 and d14. Mice receiving PBS without MDSCs were controls. Tumor volume was measured and plotted at indicated times (5 mice per group). (**D**) Flow cytometry analysis of expression of ki67 and Annexin V in gp100-specific $tetramer^+CD8^+TCRV\beta^+$ cells, and absolute number of these $tetramer^+CD8^+TCRV\beta^+$ cells per 10^6 cells in tumor infiltrates 3d after the initial MDSC transfer (5 mice per group). *, $p<0.05$; **, $p<0.01$. Data (mean ± SEM) are representative of 2 independent experiments.

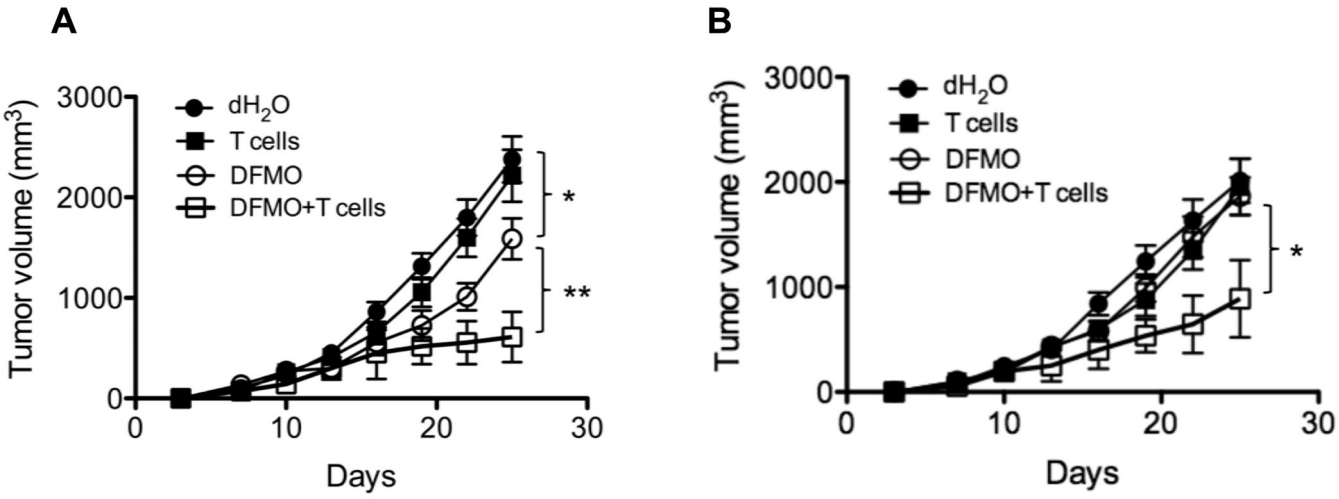

Figure 8. DFMO augments the efficacy of adoptive T cell therapy

(**A**) Mice were s.c. injected with 10^6 B16-SIY cells (5 mice per group). DFMO was administered as a 1% solution in drinking water starting 1 day after tumor injection. Mice fed with dH_2O without DFMO were used as controls. 7 days after tumor inoculation, activated SIY-specific 2C $CD8^+$ T cells were i.v. injected into tumor-bearing mice. (**B**) Mice were s.c. injected with 10^6 B16F10 cells (5 mice per group). DFMO was administered as a 1% solution in drinking water starting 7 day after tumor injection. Mice fed with dH_2O without DFMO were used as controls. Activated gp100-specific Pmel $CD8^+$ T cells were i.v. injected into tumor-bearing mice on the same day. Tumor volumes were measured every 3 days. Data (mean ± SEM) are representative of 2 independent experiments. *, $p< 0.05$; **, $p<0.01$.